

# CLASTER: Clustering with Reinforcement Learning for Zero-Shot Action Recognition

Shreyank N Gowda  
University of Edinburgh

s.narayana-gowda@sms.ed.ac.uk

Laura Sevilla-Lara  
University of Edinburgh

l.sevilla@ed.ac.uk

Frank Keller  
University of Edinburgh

frank.keller@ed.ac.uk

Marcus Rohrbach  
Facebook AI Research  
mrf@fb.com

## Abstract

Zero-shot action recognition is the task of recognizing action classes without visual examples, only with a semantic embedding which relates unseen to seen classes. The problem can be seen as learning a function which generalizes well to instances of unseen classes without losing discrimination between classes. Neural networks can model the complex boundaries between visual classes, which explains their success as supervised models. However, in zero-shot learning, these highly specialized class boundaries may not transfer well from seen to unseen classes. In this paper we propose a centroid-based representation, which clusters visual and semantic representation, considers all training samples at once, and in this way generalizing well to instances from unseen classes. We optimize the clustering using Reinforcement Learning which we show is critical for our approach to work. We call the proposed method CLASTER and observe that it consistently outperforms the state-of-the-art in all standard datasets, including UCF101, HMDB51 and Olympic Sports; both in the standard zero-shot evaluation and the generalized zero-shot learning. Further, we show that our model performs competitively in the image domain as well, outperforming the state-of-the-art in many settings.

## 1. Introduction

Research on action recognition in videos has made rapid progress in the last years, with models becoming more accurate and even some datasets becoming saturated. Much of this progress has hinged on large scale training sets. However, it is not practical to collect thousands of video samples every time we want a network to recognize a new class. This idea has led to research in the zero-shot learning (ZSL) do-

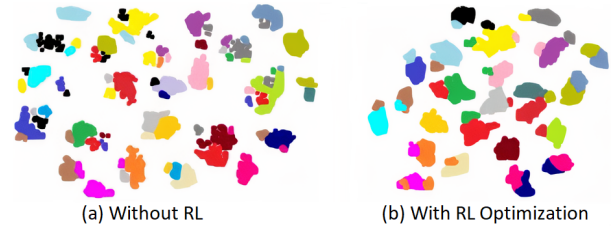


Figure 1. CLASTER improves the representation and clustering in unseen classes. The figure shows t-SNE [26] of video instances, where each color corresponds to a unique unseen class label. Our reinforcement learning (RL) optimization improves the representation by making it more compact: in (b) instances of the same class, i.e. same color, are together and there are less outliers for each class compared to (a).

main, where training occurs in a set of seen classes, and testing occurs in a set of unseen classes. In particular, in the case of video ZSL, class labels are typically “enriched” with semantic embeddings, which are sometimes manually annotated and other times inferred automatically. These semantic embeddings map the seen training classes to new unseen classes. In the typical prediction pipeline, at test time a seen class is predicted, and its semantic embedding is used to search for a nearest neighbor in the space of the semantic embeddings of unseen classes. The predicted class will be the class corresponding to the nearest neighbor. While ZSL is potentially a very useful technology, it also presents challenges.

Neural networks have proven extraordinarily powerful at learning complex discrimination functions of classes with many modes. In other words, instances of the same class can be very different and still be projected by the neural network to the same category. While this works well in supervised training, it can be a problem in zero-shot recognition, where the highly specialized discrimination function

might not transfer well to instances of unseen categories. In this work, we build a representation based on three main ideas. First, we turn to clustering, and use the centroids of the clusters to represent a video. We postulate that centroids are more robust to outliers. The initial clustering considers all training instances at once instead of optimizing the classification of single instances. Second, our representation is a combination of a visual and a semantic representation, both during clustering and when representing each instance, this allows better transfer to unseen classes.

Third, to directly use the signal from the classification supervision for clustering, we use Reinforcement Learning (RL). Specifically, we use the REINFORCE algorithm to directly update the cluster centroids. This optimization improves the clustering significantly. As we can see in Fig. 1, it leads to less noisy and more compact representations for unseen classes. We call the proposed method CLASTER, for *CLustering for Action recognition in zero-ShoT LEaRning*, and show that it significantly outperforms all existing methods across all standard zero-shot action recognition datasets and tasks. Our method also generalizes well to the image domain, showing strong performance on four datasets.

**Contributions:** Our main contribution is CLASTER, a novel model for zero-shot action recognition which learns a clustering-based representation optimized with reinforcement learning (RL). Clustering with RL has not previously been explored for this task, and we show in our ablations that the RL optimization is the critical aspect of our approach which learns a representation which generalizes better to unseen classes. In our experimental evaluation we find that CLASTER consistently outperforms recent state-of-the-art on three challenging zero-shot action recognition benchmarks, Olympics, HMDB51, and UCF101, both, in zero-shot learning and in the more challenging generalized zero-shot learning (GZSL) task.

## 2. Related Work

**Traditional Fully Supervised Action Recognition.** The seminal work of Simonyan and Zisserman [41] introduced the now standard two-stream deep learning framework, which combines spatial and temporal information. Spatio-temporal CNNs [43, 37, 5] are also widely used as backbones for many applications, including this work. More recently, research has incorporated attention [45, 15] and leveraged the multi-modal nature of videos [2]. Ji et al. [18], proposed the use of knowledge maps for coarse-to-fine action recognition.

**Zero-shot Learning.** Early approaches followed the idea of learning semantic classifiers for seen classes and then classifying the visual patterns by predicting semantic descriptions and comparing them with descriptions of unseen classes. In this space, Lampert et al. [22] propose attribute

prediction, using the posterior of each semantic description. The SJE model [1] uses multiple compatibility functions to construct a joint embedding space. ESZSL [39] uses a Frobenius norm regularizer to learn an embedding space. In videos, there are additional challenges: action labels need more complex representations than objects and hence give rise to more complex manual annotations.

**ZSL for Action Recognition.** Early work [38] was restricted to cooking activities, using script data to transfer to unseen classes. Gan et al. [12] consider each action class as a domain, and address semantic representation identification as a multi-source domain generalization problem. Manually specified semantic representations are simple and effective [56] but labor-intensive to annotate. To overcome this, the use of label embeddings has proven popular, as only category names are needed. Some approaches use common embedding space between class labels and video features [53, 52], pairwise relationships between classes [10], error-correcting codes [36], inter-class relationships [11], out-of-distribution detectors [27], and Graph Neural networks [14]. In contrast, we are learning to optimize centroids of visual semantic representations that generalize better to unseen classes.

**Reinforcement Learning for Zero-Shot Learning.** RL for ZSL in images was introduced by Liu et al. [24] by using a combination of ontology and RL. In zero-shot text classification, Ye et al. [54] propose a self-training method to leverage unlabeled data. RL has also been used in the zero-shot setting for task generalization [34], active learning [7], and video object segmentation [17]. To the best of our knowledge, there is no previous work using RL for optimizing centroids in zero-shot recognition.

**Deep Approaches to Centroid Learning for Classification.** Since our approach learns cluster centroids using RL, it is related to the popular cluster learning strategy for classification called Vector of Locally Aggregated Descriptors (VLAD) [3]. The more recent NetVLAD [3] leverages neural networks which helps outperform the standard VLAD by a wide margin. ActionVLAD [16] aggregates NetVLAD over time to obtain descriptors for videos. ActionVLAD uses clusters that correspond to spatial locations in a video while we use joint visual semantic embeddings for the entire video. In general, VLAD uses residuals with respect to cluster centroids as representation while CLASTER uses a weighting of the centroids. The proposed CLASTER outperforms NetVLAD by a large margin on both HMDB51 and UCF101.

## 3. CLASTER

We now describe the proposed method, CLASTER, which leverages clustering of visual and semantic features for video action recognition and optimizes the clustering with RL. Figure 2 shows an overview of the method.

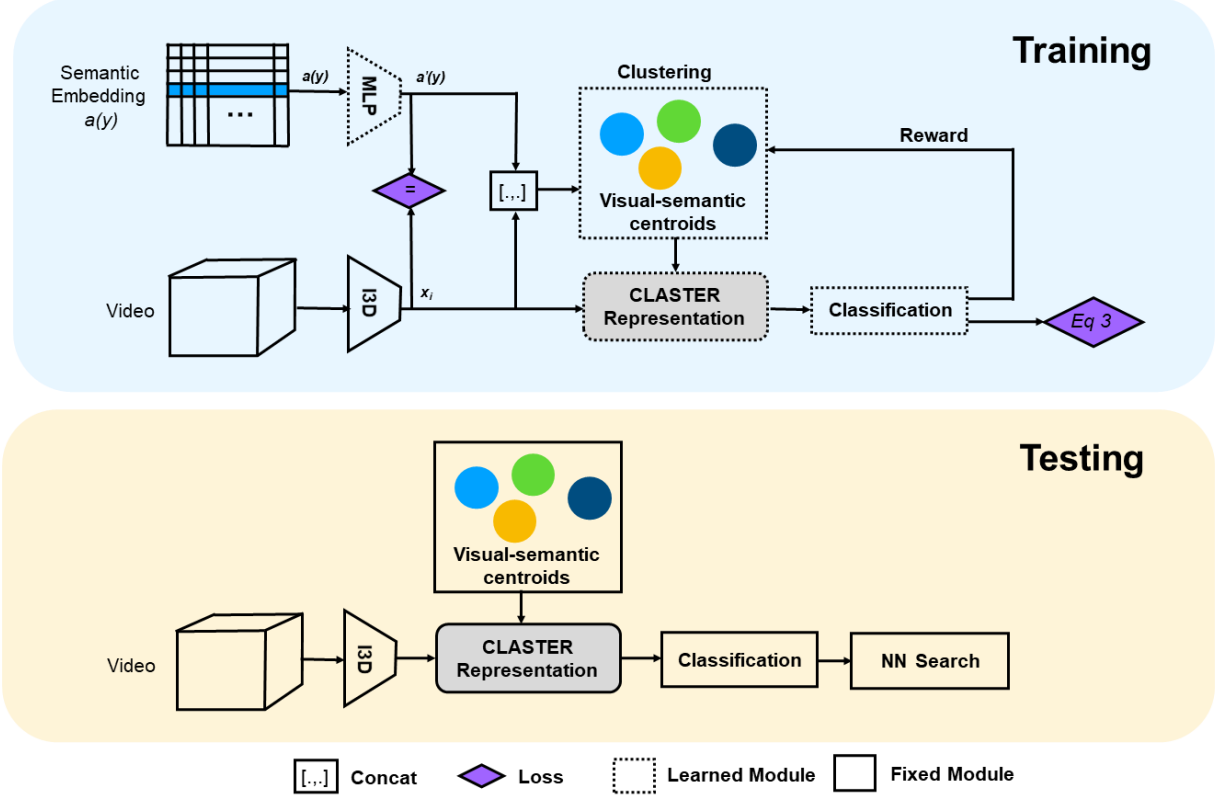


Figure 2. Overview of CLASTER. We train an MLP to map the semantic embedding to the same space as the visual features. We cluster these visual-semantic representations with k-means to obtain initial cluster centroids (Sec. 3.2). We then represent our video by a weighted representation of all clusters, which we refer to as CLASTER representation (Sec. 3.3), which is expanded in Fig. 3. This is used as input for the final classification (Sec. 3.4 and Eq. 3). Based on the classification result, we send a reward and optimize the cluster centroids using REINFORCE (Sec. 3.5). At test time, we first perform classification on the seen classes and then do a nearest neighbor (NN) search to predict the unseen class.

### 3.1. Problem Definition

Let  $S$  be the training set of seen classes.  $S$  is composed of tuples  $(x, y, a(y))$ , where  $x$  represents the spatio-temporal features of a video,  $y$  represents the class label in the set of  $Y_s$  seen class labels, and  $a(y)$  denotes the category-specific semantic representation of class  $y$ . These semantic representations are either manually annotated or computed using a language-based embedding of the category name, such as word2vec or sentence2vec.

Let  $U$  be the set composed of pairs  $(u, a(u))$ , where  $u$  is a class in the set of unseen classes  $Y_u$  and  $a(u)$  are the corresponding semantic representations. The seen classes  $Y_s$  and the unseen classes  $Y_u$  do not overlap.

In the zero-shot learning (ZSL) setting, given an input video the task is to predict a class label in the unseen classes, as  $f_{ZSL} : X \rightarrow Y_u$ . In the related generalized zero-shot learning (GZSL) setting, given an input video, the task is to predict a class label in the union of the seen and unseen classes, as  $f_{GZSL} : X \rightarrow Y_s \cup Y_u$ .

### 3.2. Cluster Initialization

We initialize the clustering of all instances in the training set  $S$  using k-means [9]. We obtain a representation for clustering which is not only aware of the visual features but also the semantic embedding. For this, we create a visual-semantic representation as follows. Given video  $i$ , we compute visual features  $x_i$  and a semantic embedding of their class  $y_i$  as  $a(y_i)$  (see Sec. 4 for details how we obtain these representations). We want to map both to an equal dimension and similar magnitude so they have a similar weight during clustering. Additionally, to reduce overfitting to the training classes and improve generalization, we learn a multi-layer perceptron (MLP) [55] which maps  $a(y_i)$  in the space of  $x_i$  with an MLP, which consists of two fully connected (FC) layers and a ReLU. This MLP is trained with a least-square embedding loss to minimize the distance between  $x_i$  and the output from the MLP, which we call  $a'(y)$ .  $x_i$  is kept fixed. Given these two representations, we concatenate  $x_i$  and  $a'(y)$  to obtain the visual-semantic

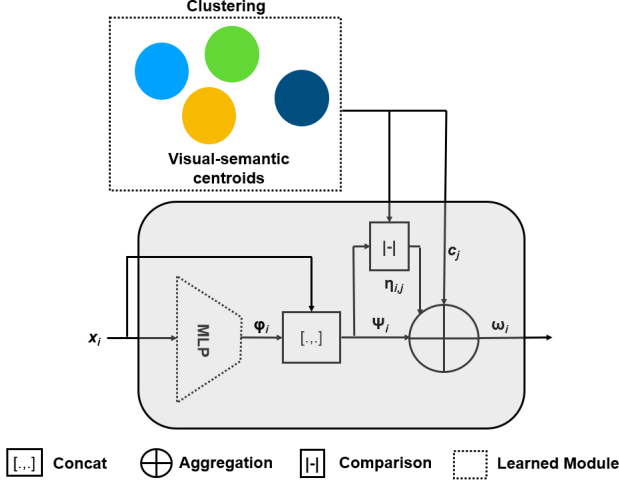


Figure 3. Our CLUSTER Representation, see Fig. 2 for the overview of the full model. The visual feature is mapped to match the space of the visual-semantic cluster centroids with an MLP and concatenation. Based on the distances to the cluster centroids the final representation  $\omega$  is a weighted representation of the centroids, more robust to the out-of-distribution instances of the unseen test classes. Details in Sec. 3.3 and Eq. 1.

representations that we cluster with k-means. Each resulting cluster  $j$  has a centroid  $c_j$ , that is the average of all visual-semantic samples in that particular cluster. Note that we keep the MLP fixed after this initial training.

### 3.3. CLUSTER Representation

We now detail how we represent videos using the clusters we computed, our *CLUSTER* representation. The intuition here is that representing data w.r.t. the visual-semantic centroids of the training set will lead to a representation which generalizes well to unseen classes. This would avoid overfitting to the training classes as it often happens with hidden representations. In other words, a representation w.r.t centroids is more robust to outliers, which is helpful since all instances of the unseen classes are effectively outliers w.r.t. the training distribution.

To classify a video  $x_i$  we first project it in the visual-semantic space of the clusters and represent it using the centroids. This CLUSTER representation is then used as input to the classification layer. Figure 3 shows this network in detail. Recall that our centroids are based on a visual *and* a semantic vector. To estimate the semantic vector, we project  $x_i$  to  $\phi_i$  with an MLP. Concatenating  $x_i$  and  $\phi_i$  we obtain the intermediate representation  $\psi_i$  which is in the same visual-semantic space as the cluster centroids. Now, to represent instance  $i$  with respect to the centroids, we compute the Euclidean distance to each cluster  $j$ , which we refer to as  $d_{i,j}$ , take its inverse  $1/d_{i,j}$  and normalize the distances using their maximum and minimum values. We

refer to these normalized values as  $\eta_{i,j}$ , and they are used as the weights of each cluster centroid in our final CLUSTER representation  $\omega_i$ :

$$\omega_i = \psi_i + \sum_{j=1}^k \eta_{i,j} c_j \quad (1)$$

Our CLUSTER representation  $\omega_i$  is the input to the classification layer, discussed next. Sec. 3.5 describes how we further optimize the centroids with RL. The implementation details of the architecture of both networks are described in Sec. 4.

### 3.4. Loss Function

Given the CLUSTER representation  $\omega$  we learn to predict a training class. We use a semantic softmax function [19], to learn a function which is aware of the semantic embedding and thus can transfer better to zero-shot classes:

$$\hat{y}_i = \frac{e^{a(y_i)^T V(\omega_i)}}{\sum_{j=1}^S e^{a(y_j)^T V(\omega_i)}}, \quad (2)$$

where  $S$  is the total number of seen classes,  $V$  is an MLP and the output  $\hat{y}_i$  is a vector with a probability distribution over the seen classes. We train a multi-class classifier, which minimizes the cross-entropy loss with a regularization term ( $W$  refers to all weights in the network):

$$\min_W \sum_{i=1}^N \mathcal{L}(x_i) + \lambda \|W\|_F^2. \quad (3)$$

### 3.5. Optimization with Reinforcement Learning

We now describe the optimization of the cluster centroids with RL. For this, we compute two variables that will determine each centroid update: the reward, which measures whether the classification is correct and will determine the direction of the update, and the classification score, which measures how far the prediction is from the correct answer and will determine the magnitude of the update.

Given the probabilistic prediction  $\hat{y}_i$  and the one-hot representation of the ground truth class  $y_i$ , we compute the classification score as the dot product of the two:  $z_i = y_i \cdot \hat{y}_i$ . To obtain the reward, we check if the maximum of  $\hat{y}_i$  and  $y_i$  lie in the same index.

$$r = \begin{cases} 1 & \text{if } \arg \max \hat{y}_i = \arg \max y_i \\ -1 & \text{otherwise} \end{cases} \quad (4)$$

This essentially gives a positive reward if the model has predicted a correct classification and a negative reward if the classification was incorrect. This formulation is inspired by Likas [23], where it is used for competitive learning.

Now we can update the cluster centroid  $c_j$  closest to  $\psi_i$  using the REINFORCE [23] algorithm.

We compute the update of  $c_j$ , which we call  $\Delta c_j$  as:

$$\Delta c_j = \alpha(r - \beta_j) \frac{\partial \ln g_j}{\partial c_j}, \quad (5)$$

where  $\alpha$  is a fixed learning rate,  $r$  is the reward,  $\beta_j$  is called the reinforcement baseline, and  $\frac{\partial \ln g_j}{\partial c_j}$  is called the characteristic eligibility of cluster centroid  $c_j$ , which quantifies the match of a cluster  $j$  with respect to a given input. This term is approximated as:

$$\frac{\partial \ln g_j}{\partial p_j} = \frac{z_i - p_j}{p_j(1 - p_j)}, \quad (6)$$

and  $p_j = 2(1 - f(\eta_{i,j}))$  and  $f(x) = \frac{1}{1+e^{-x}}$ . Substituting Eq. 6 in Eq. 5, we obtain:

$$\Delta c_j = \alpha(r - \beta_j) \frac{\partial \ln g_j}{\partial p_j} \frac{\partial p_j}{\partial \eta_{i,j}} \frac{\partial \eta_{i,j}}{\partial c_j}. \quad (7)$$

From Eq. 6 and the definition of  $p_j$ , we get to:

$$\Delta c_j = \alpha(r - \beta_j)(z_i - p_j) \frac{\partial \eta_{i,j}}{\partial c_j}. \quad (8)$$

Using Euclidean distance and setting  $\beta_j$  to zero, the updating rule for cluster centroid  $c_j$  is:

$$\Delta c_j = \alpha r (z_i - p_j) (\psi_i - c_j). \quad (9)$$

For further details on this derivation, please refer to Likas [23]. The main difference is that we do not consider our clusters to be Bernoulli units, where the modification of the cluster representative is discrete (either 0 or 1). Instead, we modify the cluster centroid with  $z_i$ , which is continuous between 0 and 1.

### 3.6. Use of Sentence2vec

Some datasets, such as HMDB51 [21], do not have semantic manual annotations. Thus, semantic representations are often computed using a word2vec model [29]. In most action recognition datasets, labels are phrases (e.g. “playing guitar”) and thus the semantic embeddings are computed by averaging the word2vec embeddings of each word. This works in some cases, however, simple averaging does not always capture the inter-dependency of action classes. For example, “horse riding” and “horse racing” lie far apart in the word2vec space.

To alleviate this, we propose using sentence2vec [35], a model designed to capture the meaning of sentences. Specifically, sentence2vec learns embeddings with respect to the sentence context. It represents the sentence context as n-grams and optimizes the additive combination of the

word vectors to obtain sentence embeddings. Figure 4 illustrates how class neighbors become more meaningful when we move from word2vec to sentence2vec.

We show in Sec. 5.5 and 5.6 that sentence2vec significantly improves performance of some of the recent state-of-the-art approaches, reaching performance close to using manual semantic representation. This suggests the potential of sentence2vec to automatically annotate large scale datasets. We also observe that combining multiple of these embeddings (e.g., through averaging) leads to a small but consistent improvement, suggesting they may contain complementary information.

## 4. Implementation Details

**Visual features.** We use RGB and flow features extracted from the *Mixed 5c* layer of an I3D network pre-trained on the Kinetics [5] dataset. The *Mixed 5c* output of the flow network is averaged across the temporal dimension and pooled by four in the spatial dimension and then flattened to a vector of size 4096. We then concatenate the two. In the case of images, similar to other approaches, we use 2048D ResNet101 features, pre-trained on Imagenet [6].

**Network architecture.** The MLP in the CLUSTER Representation module is a two-layer FC network, whose output after concatenation with the video feature has the same dimensions as the cluster representatives. The size of the FC layers is 8192 each. The final classification MLP (represented as a classification block in Figure 2) consists of two convolutional layers and two FC layers, where the last layer equals the number of unseen classes in the dataset we are looking at. All the modules are trained with the Adam optimizer with a learning rate of 0.0001 and weight decay of 0.0005.

**Number of clusters.** Since the number of clusters is a hyperparameter, we evaluate the effect of the number of clusters on the UCF101 dataset for videos and choose 6 after the average performance stabilizes as can be seen in the supplementary material. We then use the same number for the HMDB51 and Olympics datasets. Similarly we test the effect of cluster numbers on the SUN dataset for images and use 9 clusters for all image datasets based on this.

**RL optimization.** We use 10,000 iterations and the learning rate  $\alpha$  is fixed to 0.1 for the first 1000 iterations, 0.01 for the next 1000 iterations and then drop it to 0.001 for the remaining iterations.

**Semantic embeddings.** We experiment with three types of embeddings as semantic representations of the classes. We have human annotated semantic representations for UCF101 and the Olympic sports dataset of sizes 40 and 115 respectively. HMDB51 does not have human annotated semantic representations. Instead, we use a skip-gram model trained on the news corpus provided by Google to generate word2vec embeddings. Using action classes as input,



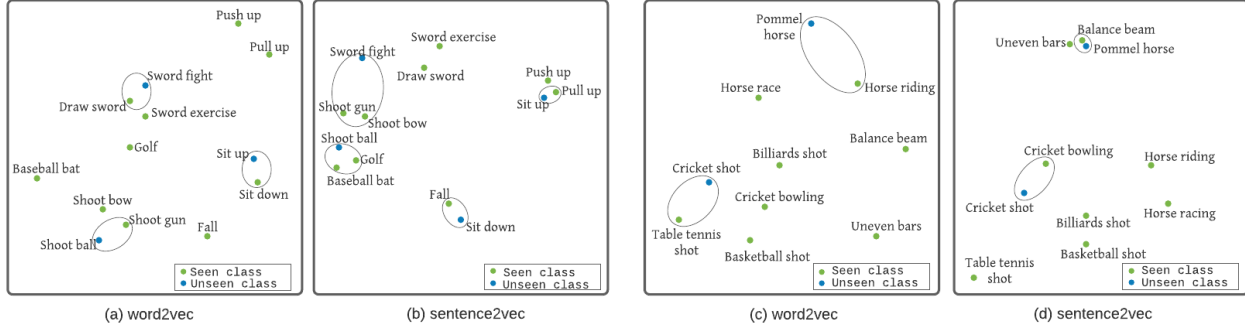


Figure 4. **HMDB51** (a) Averaging word embeddings can produce poor results in certain cases. For example the nearest neighbor of “shoot ball” is “shoot gun”, and of “sit up” is “sit down” which are not necessarily meaningful (b) Sentence2vec better captures phrase meanings: Nearest neighbors to “sit up” is now “push up”, and for “shoot ball”, is golf. **UCF101** (c) The same effect is observed, where after averaging word2vec representations, the nearest neighbor of “pommel horse” is “horse riding” (d) Sentence2vec helps capture phrase meanings: the while nearest neighbor of “pommel horse” is now “balance beam”. The circles contain the nearest neighbor to the given unseen class and is for illustration purposes.

we obtain a vector representation of 300 dimensions. Some class labels contain multiple words. In those cases, we use the average of the word2vec embeddings. We also use sentence2vec embeddings, trained on Wikipedia. These can be obtained for both single words and multi-word expressions. In case of images, we use only the manual annotations as features since they are the best performing embedding in recent approaches.

**Rectification of the Semantic Embedding** Sometimes, in ZSL, certain data points tend to appear as nearest-neighbor of many other points in the projection space. This is referred to as the hubness problem [40]. We avoid this problem using semantic rectification [25], where the class representation is modified by averaging the output generated by the projection network, which in our case is the penultimate layer of the classification MLP. Specifically, for the unseen classes, we perform rectification by first using the MLP trained on the seen classes to project the semantic embedding to the visual space. We add the average of projected semantic embeddings from the k-nearest neighbors of the seen classes, specifically as follows:

$$\hat{a}(y_i) = a'(y_i) + \frac{1}{k} \sum_{n \in N} \cos(a'(y_i), n) \cdot n, \quad (10)$$

where  $a'(y)$  refers to the embedding after the MLP introduced in Sec. 3.2,  $\cos(a, n)$  refers to the cosine similarity between  $a$  and  $n$ , the operator  $\cdot$  refers to the dot product and  $N$  refers to the k-nearest neighbors of  $a'(y_{u_i})$ .

**Nearest Neighbor Search** At test time in the ZSL, given a test video, we predict a seen class and compute or retrieve its semantic representation. After rectification, we find the nearest neighbor in the set of unseen classes. In the GZSL task, class predictions may be of seen or unseen classes. Thus, we first use a bias detector [13] which helps us detect

if the video belongs to the seen or unseen class. If it belongs to a seen class, we predict the class directly from our model, else we proceed as in ZSL.

## 5. Experimental Analysis

In this section, we look at the qualitative and quantitative performance of our model. We first describe the experimental settings, and then show an ablation study, that explores the contribution of each component. We then compare the proposed method to the state-of-the-art in the ZSL and GZSL tasks, and give analytical insights into the advantages of CLUSTER.

### 5.1. Datasets

We choose the Olympic Sports [33], HMDB-51 [21] and UCF-101 [42], so that we can compare to recent state-of-the-art models [12, 27, 36]. We follow the commonly used 50/50 splits of Xu et al. [52], where 50 percent are seen classes and 50 are unseen classes. Similar to previous approaches [56, 12, 36, 28, 20], we report average accuracy and standard deviation over 10 independent runs. For images, we use CUB [44], SUN [50], AWA2 [47] and APY [8]. We report results on the split proposed by [47], in the standard inductive setting.

### 5.2. Ablation Study

We test the performance of using the different components of CLUSTER in Table 1. We consider no clustering (which in our case is the equivalent of having a single cluster), random clustering and the standard k-means. We observe that using clusters is beneficial, but only if they are meaningful, as in the case of k-means.

We observe that using semantic embedding rectification (+R) improves the accuracy, as the chances of reaching previously unreachable classes increases. Next we replace the

Component	HMDB51	Olympics	UCF101
No clustering	25.6 $\pm$ 2.8	57.7 $\pm$ 3.1	31.6 $\pm$ 4.6
Random clustering (K=6)	20.2 $\pm$ 4.2	55.4 $\pm$ 3.1	24.1 $\pm$ 6.3
k-means (K=6)	27.9 $\pm$ 3.7	58.6 $\pm$ 3.5	35.3 $\pm$ 3.9
k-means + R	29.3 $\pm$ 3.8	59.4 $\pm$ 2.9	37.1 $\pm$ 2.7
k-means + R + SS	29.6 $\pm$ 3.5	59.5 $\pm$ 2.6	37.5 $\pm$ 3.2
CLUSTER w/o RL	30.1 $\pm$ 3.4	60.5 $\pm$ 1.9	39.1 $\pm$ 3.2
CLUSTER w/ NetVLAD	33.2 $\pm$ 2.8	62.6 $\pm$ 4.1	41.7 $\pm$ 3.8
CLUSTER	<b>36.8 <math>\pm</math> 4.2</b>	<b>63.5 <math>\pm</math> 4.4</b>	<b>46.4 <math>\pm</math> 5.1</b>

Table 1. Results of the ablation study of different components of CLUSTER ZSL. Each cell shows the average accuracy and the standard deviation over 5 independent runs. The study shows the effect of using a standard clustering algorithm, rectification of semantic embeddings (“R”), and replacing the standard softmax with semantic softmax. Finally, the last row represents the proposed model. All the reported accuracies are on the same five splits, note that Table 3 is with 10 splits.

standard softmax with the semantic softmax (+SS), which results in a small increase in accuracy.

Since we use RL optimization to learn cluster centroids, we compare our full model (CLUSTER) to a baseline where the centroids are updated using standard SGD instead of RL (referred to in Table 1 as “CLUSTER w/o RL”). As a comparison, we also replace our centroid-learning with NetVLAD [3]. The input to NetVLAD are also the joint visual-semantic features. We see that our model outperforms NetVLAD by an average of 4.7% and the CLUSTER w/o RL by 7.3% on the UCF101 dataset. One reason for this difference is that the loss is back-propagated through multiple parts of the model before reaching the centroids. However, with RL the centroids are directly updated using the reward signal. We see that the cluster optimization with RL gives a clear performance improvement. Section 5.7 explores how the clusters change after this optimization. In a nutshell, the RL optimization essentially makes the clusters cleaner moving most instances in a class to the same cluster.

### 5.3. Number of Clusters

We test using different number of clusters on the UCF-101 dataset and show the results in Figure 5. These are for 5 runs on random splits. As we can see, the average accuracy increases until 6 clusters, and after that remains more or less constant. Thus, we use 6 clusters and continue with the same number for both HMDB51 and Olympics. For images, similarly, we used 5 random splits of CUB and found the performance stabilizes after having 9 clusters and use the same number of clusters for the other image datasets.

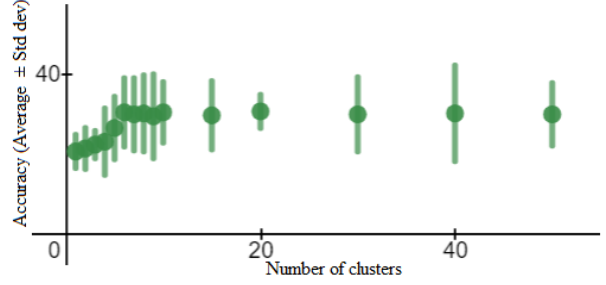


Figure 5. Effect of using different number of clusters. The green line represents the standard deviation. The reported accuracy is on the UCF101 dataset. As can be seen, the average cluster accuracy increases till about 6 clusters and then remains more or less constant. The vertical lines correspond to the standard deviation.

Component	CUB	SUN	AWA	APY
No clustering	61.2	54.6	62.8	33.6
Random clustering (K=9)	56.6	48.3	56.9	28.2
k-means (K=9)	68.9	60.1	68.8	37.9
k-means + R	69.5	61.2	69.4	38.3
k-means + R + SS	69.8	61.4	69.8	38.5
CLUSTER w/o RL	71.4	63.2	70.9	39.3
CLUSTER w/ NetVLAD	73.1	64.7	71.8	41.2
CLUSTER	<b>76.4</b>	<b>67.2</b>	<b>74.1</b>	<b>44.1</b>

Table 2. Results of the ablation study on image datasets of different components of CLUSTER ZSL. Each cell shows the average unseen class accuracy over 5 independent runs. The study shows the effect of using a standard clustering algorithm, rectification of semantic embeddings (“R”), and replacing the standard softmax with semantic softmax. Finally, the last row represents the proposed model. All the reported accuracies are on the proposed split [48].

### 5.4. Ablation Study on Image Datasets

In Table 2 we show the ablation results on the proposed splits of the CUB, SUN, AWA and APY datasets. The results are consistent with those reported on the paper for ablation on video datasets. Again, we can see that optimizing the visual-semantic centroids with REINFORCE yields best results with a consistent improvement over NetVLAD and optimizing with backpropagation.

### 5.5. Results on ZSL

We compare our approach to several state-of-the-art methods: the out-of-distribution detector method (OD) [27], a generative approach to zero-shot action recognition (GGM) [31], the evaluation of output embeddings (SJE) [1], the feature generating networks (WGAN) [46], the end-to-end training for realistic applications approach (E2E) [4], the inverse autoregressive flow (IAF) based generative model, bi-directional adversarial GAN (Bi-dir GAN) [30] and prototype sampling graph neural network (PS-

Method	SE	Olympics	HMDB51	UCF101
SJE [1]	M	47.5 ± 14.8	-	12.0 ± 1.2
Bi-Dir GAN [30]	M	53.2 ± 10.5	-	24.7 ± 3.7
IAF [30]	M	54.9 ± 11.7	-	26.1 ± 2.9
GGM [31]	M	57.9 ± 14.1	-	24.5 ± 2.9
OD [27]	M	65.9 ± 8.1	-	38.3 ± 3.0
WGAN [46]	M	64.7 ± 7.5	-	37.5 ± 3.1
<b>CLASTER (ours)</b>	M	<b>67.4 ± 7.8</b>	-	<b>51.8 ± 2.8</b>
SJE [1]	W	28.6 ± 4.9	13.3 ± 2.4	9.9 ± 1.4
IAF [30]	W	39.8 ± 11.6	19.2 ± 3.7	22.2 ± 2.7
Bi-Dir GAN [30]	W	40.2 ± 10.6	21.3 ± 3.2	21.8 ± 3.6
GGM [31]	W	41.3 ± 11.4	20.7 ± 3.1	20.3 ± 1.9
WGAN [46]	W	47.1 ± 6.4	29.1 ± 3.8	25.8 ± 3.2
OD [27]	W	50.5 ± 6.9	30.2 ± 2.7	26.9 ± 2.8
PS-GNN [14]	W	61.8 ± 6.8	32.6 ± 2.9	43.0 ± 4.9
E2E [4]*	W	61.4 ± 5.5	33.1 ± 3.4	46.2 ± 3.8
<b>CLASTER (ours)</b>	W	<b>63.8 ± 5.7</b>	<b>36.6 ± 4.6</b>	<b>46.7 ± 5.4</b>
WGAN*	S	46.8 ± 4.2	34.7 ± 4.3	32.8 ± 5.4
OD*	S	50.8 ± 2.1	39.3 ± 3.1	45.7 ± 2.3
<b>CLASTER (ours)</b>	S	<b>64.2 ± 3.3</b>	<b>41.8 ± 2.1</b>	<b>50.2 ± 3.8</b>
<b>CLASTER (ours)</b>	C	<b>67.7 ± 2.7</b>	<b>42.6 ± 2.6</b>	<b>52.7 ± 2.2</b>

Table 3. Results on ZSL. SE: semantic embedding, M: manual representation, W: word2vec embedding, S: sentence2vec, C: Combination of embeddings. \* run by us with author’s code on same splits as ours.

GNN) [14]. We use a pre-trained model on Kinetics.

We observe that the proposed CLASTER consistently outperforms other state-of-the-art approaches. Results are shown in Table 3. On the HMDB51 dataset, it improves 3.5% over the next best performing model E2E [4]. On UCF101 it improves 13.5% over the next best performing model, when using semantic manual annotations.

On the Olympics dataset, CLASTER improves 1.5% over the next best performing model OD [27] when using manual semantic representations; and 2% over PS-GNN [14] when using word2vec.

We measure the impact of using sentence2vec instead of word2vec. We test this on our own method, as well as as input to OD and WGAN, using the authors’ code. We show that sentence2vec significantly improves over using word2vec, especially on UCF101 and HMDB51. Combination of embeddings resulted in average improvements of 0.3%, 0.8% and 0.9% over the individual best performing embedding of CLASTER.

## 5.6. Results on GZSL

We now compare to the same approaches in the GZSL task in Table 4, the reported results are the harmonic mean of the seen and unseen class accuracies. Here CLASTER outperforms all previous methods across different modalities. We obtain an improvement on average of 2.6% and 5% over the next best performing method on the Olympics

Method	SE	Olympics	HMDB51	UCF101
Bi-Dir GAN [30]	M	44.2 ± 11.2	-	22.7 ± 2.5
IAF [30]	M	48.4 ± 7.0	-	25.9 ± 2.6
GGM [31]	M	52.4 ± 12.2	-	23.7 ± 1.2
WGAN [46]	M	59.9 ± 5.3	-	44.4 ± 3.0
OD[27]	M	66.2 ± 6.3	-	49.4 ± 2.4
<b>CLASTER (ours)</b>	M	<b>68.8 ± 6.6</b>	-	<b>50.9 ± 3.2</b>
IAF [30]	W	30.2 ± 11.1	15.6 ± 2.2	20.2 ± 2.6
Bi-Dir GAN [30]	W	32.2 ± 10.5	7.5 ± 2.4	17.2 ± 2.3
SJE [1]	W	32.5 ± 6.7	10.5 ± 2.4	8.9 ± 2.2
GGM[31]	W	42.2 ± 10.2	20.1 ± 2.1	17.5 ± 2.2
WGAN [46]	W	46.1 ± 3.7	32.7 ± 3.4	32.4 ± 3.3
PS-GNN [14]	W	52.9 ± 6.2	24.2 ± 3.3	35.1 ± 4.6
OD [27]	W	53.1 ± 3.6	36.1 ± 2.2	37.3 ± 2.1
<b>CLASTER (ours)</b>	W	<b>58.1 ± 2.4</b>	<b>42.4 ± 3.6</b>	<b>42.1 ± 2.6</b>
WGAN*	S	47.6 ± 4.2	38.2 ± 4.1	40.2 ± 5.1
OD*	S	54.1 ± 2.7	42.3 ± 3.1	45.7 ± 2.3
<b>CLASTER (ours)</b>	S	<b>58.7 ± 3.1</b>	<b>47.4 ± 2.8</b>	<b>48.3 ± 3.1</b>
<b>CLASTER (ours)</b>	C	<b>69.1 ± 5.4</b>	<b>48.0 ± 2.4</b>	<b>51.3 ± 3.5</b>

Table 4. GZSL. SE: semantic embedding, M: manual representation, W: word2vec embedding, S: sentence2vec, C: combination of embeddings. \* run by us with author’s code. Reported results are the harmonic mean of seen and unseen class accuracies.

dataset using manual representations and word2vec respectively. We obtain an average improvement of 6.3% over the next best performing model on the HMDB51 dataset using word2vec. We obtain an improvement on average performance by 1.5% and 4.8% over the next best performing model on the UCF101 dataset using manual representations and word2vec respectively. Similarly to ZSL, we show generalized performance improvements using sentence2vec. We also report results on the combination of embeddings. We see an improvement of 0.3%, 0.6% and 0.4% over the individual best embedding for CLASTER.

## 5.7. Analysis of the RL optimization

We analyze how RL affects clustering on the UCF101 training set. For each class in the training set, we measure the distribution of clusters that they belong to, visualized in the supplementary material. We observe that after the RL optimization, the clustering becomes “cleaner”. This is, most instances in a class belong to a dominant cluster. This effect can be measured using the purity of the cluster:

$$Purity = \frac{1}{N} \sum_{i=1}^k max_j |c_i \cap t_j|, \quad (11)$$

where  $N$  is the number of data points (video instances),  $k$  is the number of clusters,  $c_i$  is a cluster in the set of clusters, and  $t_j$  is the class which has the maximum count for cluster  $c_i$ . Poor clustering results in purity values close to 0, and a perfect clustering will return a purity of 1. Using



Method	CUB		SUN		AWA2		APY	
	ZSL	GZSL	ZSL	GZSL	ZSL	GZSL	ZSL	GZSL
SJE [1]	53.9	33.6	53.7	19.8	61.9	14.4	32.9	6.9
WGAN [46]	57.3	52.3	60.8	40.0	68.2	60.2	-	-
VAEGAN [49]	72.9	68.9	65.6	43.1	70.3	65.2	-	-
LEF [32]	74.3	<b>70.7</b>	66.7	<b>46.3</b>	73.4	66.7	-	-
R-PRR [51]	75.0	64.7	63.4	36.2	72.5	69.7	43.9	36.3
RGEM [51]	76.1	66.1	63.8	36.8	73.6	71.5	<b>44.4</b>	37.2
<b>CLUSTER</b>	<b>76.4</b>	69.8	<b>67.2</b>	44.8	<b>74.1</b>	<b>72.7</b>	44.1	<b>40.8</b>

Table 5. Results on image datasets. For ZSL, we report the mean class accuracy and for GZSL, we report the harmonic mean of seen and unseen class accuracies. All approaches use manual annotations as the form of semantic embedding.

k-means, the purity of the clusters is 0.77, while optimizing the clusters with RL results in a purity of 0.89.

Finally, we observe another interesting side effect of clustering. Some of the most commonly confused classes before clustering (e.g. “Baby crawling” vs. “Mopping floor”, “Breaststroke” vs. “front crawl”, “Rowing vs. front crawl”) are assigned to different clusters after RL, resolving confusion. This suggests that clusters are also used as a means to differentiate between similar classes.

## 5.8. Results on Images

Our method also generalizes to the image domain as shown in Table 5. CLUSTER outperforms previous work in five out of eight tasks and obtains comparable results in the remaining three tasks. We compare our approach to several state-of-the-art methods: Region Graph Embedding Network with the Parts Relation Reasoning branch (RGEM) and without the branch (R-PRR) [51], the evaluation of output embeddings (SJE) [1], the feature generating networks (WGAN) [46], the feature generating framework (VAEGAN) [49] and the latent embedding feedback method (LEF) [32]. [51]).

## 5.9. Seen and Unseen Class Performance for GZSL

In order to better analyze performance of the model on GZSL, we report the average seen and unseen accuracies along with their harmonic mean. The results using different embeddings and on the UCF101, HMDB51 and Olympics datasets are reported in Table 7.

Similarly we report results on CUB, AWA2, APY and SUN and this can be seen in Table 6.

## 5.10. Change in Clusters After RL

How do the clusters change after the RL optimization? For each class in the training set, we measure the distribution of clusters that they belong to, visualized in Figure 6. Here, each column represents a class, and each color a cluster. In a perfect clustering, each column would have a single

color. We observe that after the RL optimization, the clustering becomes “cleaner”. This is, most instances in a class belong to a dominant cluster.

## 6. Statistical Significance

We consider the dependent t-test for paired samples. This test is utilized in the case of dependent samples, in our case different model performances on the same random data split. This is a case of a paired difference test. This is calculated as shown in Eq 12.

$$t = \frac{\bar{X}_D - \mu_0}{s_D / \sqrt{n}} \quad (12)$$

Where  $\bar{X}_D$  is the average of the difference between all pairs and  $s_D$  is the standard deviation of the difference between all pairs. The constant  $\mu_0$  is zero in case we wish to test if the average of the difference is different;  $n$  represents the number of samples,  $n = 10$  in our case. The comparisons can be seen in Table 8. The lower the value of ‘p’, higher the significance.

As we can see, our results are statistically significant in comparison to both OD [27] and WGAN [46] in both ZSL and GZSL. We also see that our results are statistically significant for both HMDB51 and Olympics in comparison to E2E [4]. In GZSL, OD [27] also achieves results that are significantly different in comparison to WGAN [46].

## 7. Average of Differences in Performance for Same Splits

Since the performance of the model varies for each random split (as witnessed by the standard deviation values), we average the difference in performance between CLUSTER, OD, WGAN and E2E on the same splits. We believe that this gives us a better metric to check the performance of CLUSTER with the other approaches. The results are depicted in Table 9.

## 8. Conclusion

Zero-shot action recognition is the task of recognizing action classes without any visual examples. The challenge is to map the knowledge of seen classes at training time to that of novel unseen classes at test time. We propose a novel model that learns clustering-based representation optimized by reinforcement learning. Our method consistently outperforms prior work, regardless of the semantic embeddings used, the dataset, and, both, for standard and for generalized zero-shot evaluation (GZSL). We also show that better semantic representations of action classes can be obtained using sentence2vec instead of word2vec, as the former is specifically trained to capture the meaning of multi-word expression such as the labels of action classes. Over-

Model	CUB			SUN			AWA2			APY		
	u	s	H	u	s	H	u	s	H	u	s	H
WGAN [46]	43.7	57.7	49.7	42.6	36.6	39.4	57.9	61.4	59.6	—	—	—
R-PRR [51]	61.4	68.5	64.7	42.7	31.5	36.2	64.1	76.4	69.7	29.2	48.0	36.3
RGEn [51]	60.0	73.5	66.1	44.0	31.7	36.8	67.1	76.5	71.5	30.4	48.1	37.2
CLUSTER	66.3	73.8	69.8	55.2	37.7	44.8	68.8	77.1	72.7	33.7	51.9	40.8

Table 6. Seen and unseen accuracies for CLUSTER on different datasets compared against recent state-of-the-art approaches. 'u', 's' and 'H' corresponds to average unseen accuracy, average seen accuracy and the harmonic mean of the two.

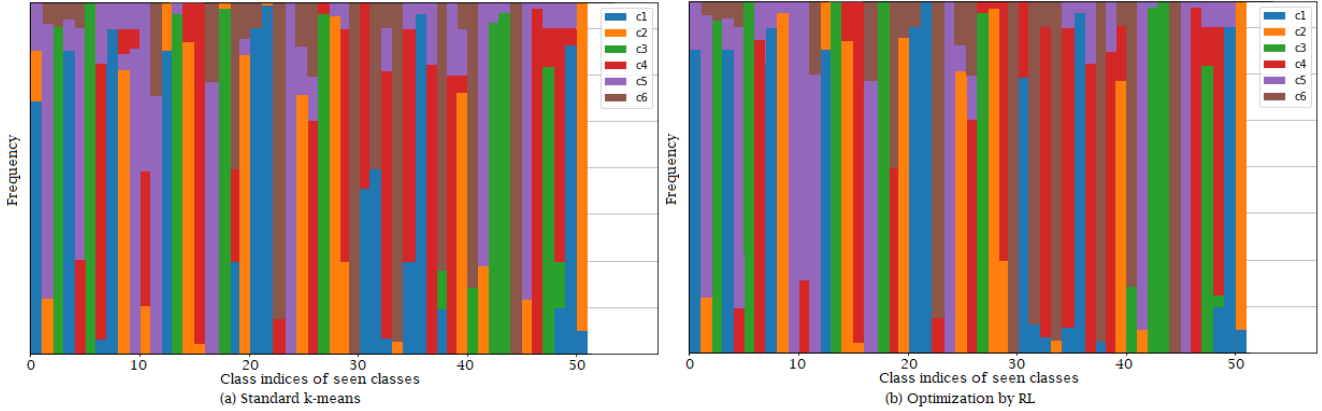


Figure 6. Analysis of how RL optimization changes the cluster to which an instance belongs. The frequencies are represented as percentages of instances in each cluster. We can see that the clusters are a lot "cleaner" after the optimization by RL.

Model	E	Olympics			HMDB51			UCF-101		
		u	s	H	u	s	H	u	s	H
WGAN [46]	A	50.8	71.4	59.4	-	-	-	30.4	83.6	44.6
OD [27]	A	61.8	71.1	66.1	-	-	-	36.2	76.1	49.1
CLUSTER	A	66.2	71.7	68.8	-	-	-	40.2	69.4	50.9
WGAN [46]	W	35.4	65.6	46.0	23.1	55.1	32.5	20.6	73.9	32.2
OD [27]	W	41.3	72.5	52.6	25.9	55.8	35.4	25.3	74.1	37.7
CLUSTER	W	49.2	71.1	58.1	35.5	52.8	42.4	30.4	68.9	42.1
WGAN [46]	S	36.1	66.2	46.7	28.6	57.8	38.2	27.5	74.7	40.2
OD [27]	S	42.9	73.5	54.1	33.4	57.8	42.3	32.7	75.9	45.7
CLUSTER	S	49.9	71.3	58.7	42.7	53.2	47.4	36.9	69.8	48.3
CLUSTER	C	66.8	71.6	69.1	43.7	53.3	48.0	40.8	69.3	51.3

Table 7. Seen and unseen accuracies for CLUSTER on different datasets using different embeddings. 'E' corresponds to the type of embedding used, wherein 'A', 'W', 'S' and 'C' refers to manual annotations, word2vec, sen2vec and combination of the embeddings respectively. 'u', 's' and 'H' corresponds to average unseen accuracy, average seen accuracy and the harmonic mean of the two. All the reported results are on the same splits.

all, we achieve remarkable improvements over the previously reported results, up to 11.9% absolute improvement on HMDB51 for GZSL. We also show that our method generalizes to the image domain as well.

## References

- [1] Zeynep Akata, Scott Reed, Daniel Walter, Honglak Lee, and Bernt Schiele. Evaluation of output embeddings for fine-grained image classification. In *Proceedings of the IEEE conference on computer vision and pattern recognition*, pages 2927–2936, 2015. 2, 7, 8, 9
- [2] Humam Alwassel, Dhruv Mahajan, Lorenzo Torresani, Bernard Ghanem, and Du Tran. Self-supervised learning by cross-modal audio-video clustering. *arXiv preprint arXiv:1911.12667*, 2019. 2
- [3] Relja Arandjelovic, Petr Gronat, Akihiko Torii, Tomas Pa-jdla, and Josef Sivic. Netvlad: Cnn architecture for weakly supervised place recognition. In *Proceedings of the IEEE conference on computer vision and pattern recognition*, pages 5297–5307, 2016. 2, 7
- [4] Biagio Brattoli, Joseph Tighe, Fedor Zhdanov, Pietro Per-ona, and Krzysztof Chalupka. Rethinking zero-shot video classification: End-to-end training for realistic applications. In *Proceedings of the IEEE/CVF Conference on Computer Vision and Pattern Recognition*, pages 4613–4623, 2020. 7, 8, 9, 11
- [5] J. Carreira and Andrew Zisserman. Quo vadis, action recog-nition? a new model and the kinetics dataset. In *IEEE Conf. Comput. Vis. Pattern Recog.*, 2017. 2, 5
- [6] Jia Deng, Wei Dong, Richard Socher, Li-Jia Li, Kai Li, and Li Fei-Fei. Imagenet: A large-scale hierarchical image database. In *2009 IEEE conference on computer vision and pattern recognition*, pages 248–255. Ieee, 2009. 5

Pairs	Dataset	t-value	Statistical significance( $p < 0.05$ )	Type
CLUSTER and OD [27]	UCF101	-15.77	Significant, $p < 0.00001$	ZSL
CLUSTER and WGAN [46]	UCF101	-9.08	Significant, $p < 0.00001$	ZSL
CLUSTER and E2E [4]	UCF101	-0.67	Not Significant, $p = 0.26$	ZSL
OD [27] and WGAN [46]	UCF101	-1.70	Not Significant, $p = 0.12278$	ZSL
CLUSTER and OD [27]	HMDB51	-4.33	Significant, $p = 0.00189$	ZSL
CLUSTER and WGAN [46]	HMDB51	-5.54	Significant, $p = 0.00036$	ZSL
CLUSTER and E2E [4]	HMDB51	-3.77	Significant, $p = 0.00219$	ZSL
OD [27] and WGAN [46]	HMDB51	-3.71	Significant, $p = 0.00483$	ZSL
CLUSTER and OD [27]	Olympics	-9.06	Significant, $p < 0.00001$	ZSL
CLUSTER and WGAN [46]	Olympics	-11.73	Significant, $p < 0.00001$	ZSL
CLUSTER and E2E [4]	Olympics	-2.72	Significant, $p = 0.012$	ZSL
OD [27] and WGAN [46]	Olympics	-2.47	Significant, $p = 0.03547$	ZSL
CLUSTER and OD [27]	UCF101	-4.51	Significant, $p = 0.00148$	GZSL
CLUSTER and WGAN [46]	UCF101	-5.49	Significant, $p = 0.00039$	GZSL
OD [27] and WGAN [46]	UCF101	-3.16	Significant, $p = 0.01144$	GZSL
CLUSTER and OD [27]	HMDB51	-5.08	Significant, $p = 0.00066$	GZSL
CLUSTER and WGAN [46]	HMDB51	-7.51	Significant, $p = 0.00004$	GZSL
OD [27] and WGAN [46]	HMDB51	-5.27	Significant, $p = 0.00051$	GZSL
CLUSTER and OD [27]	Olympics	-5.79	Significant, $p = 0.00026$	GZSL
CLUSTER and WGAN [46]	Olympics	-8.39	Significant, $p = 0.00002$	GZSL
OD [27] and WGAN [46]	Olympics	-6.22	Significant, $p = 0.00014$	GZSL

Table 8. Comparison of the t-test for different pairs of models on the same random split. Lower the value of 'p', higher the significance. As we can see, our results are statistically significant in comparison to both OD [27] and WGAN [46] in both ZSL and GZSL. For GZSL, OD [27] also achieves results that are significant in comparison to WGAN [46].

Models	Setting	Olympics	HMDB51	UCF101
Ours and WGAN [46]	ZSL	$17.5 \pm 4.5$	$7.0 \pm 3.8$	$17.4 \pm 5.7$
Ours and OD [27]	ZSL	$13.6 \pm 4.5$	$2.4 \pm 1.6$	$14.3 \pm 2.7$
Ours and E2E [4]	ZSL	$2.6 \pm 2.8$	$3.7 \pm 2.8$	$0.4 \pm 1.8$
Ours and WGAN [46]	GZSL	$11.2 \pm 4.0$	$9.3 \pm 3.7$	$8.1 \pm 4.4$
Ours and OD [27]	GZSL	$4.6 \pm 2.4$	$5.2 \pm 3.1$	$2.7 \pm 1.8$

Table 9. Comparing the average of the difference in performance for recent state-of-the-art approaches in zero-shot and generalized zero-shot action recognition on the same splits. All results were computed using sen2vec as the embedding. We can see that we outperform recent approaches in every scenario.

- [7] Yang Fan, Fei Tian, Tao Qin, Jiang Bian, and Tie-Yan Liu. Learning what data to learn. *arXiv preprint arXiv:1702.08635*, 2017. 2
- [8] Ali Farhadi, Ian Endres, Derek Hoiem, and David Forsyth. Describing objects by their attributes. In *2009 IEEE Conference on Computer Vision and Pattern Recognition*, pages 1778–1785. IEEE, 2009. 6
- [9] Edward W Forgy. Cluster analysis of multivariate data: efficiency versus interpretability of classifications. *biometrics*, 21:768–769, 1965. 3
- [10] Chuang Gan, Ming Lin, Yi Yang, Gerard De Melo, and Alexander G Hauptmann. Concepts not alone: Exploring pairwise relationships for zero-shot video activity recognition. In *Thirtieth AAAI conference on artificial intelligence*, 2016. 2
- [11] Chuang Gan, Ming Lin, Yi Yang, Yueting Zhuang, and Alexander G Hauptmann. Exploring semantic inter-class relationships (sir) for zero-shot action recognition. In *Proceedings of the National Conference on Artificial Intelligence*, 2015. 2
- [12] Chuang Gan, Tianbao Yang, and Boqing Gong. Learning attributes equals multi-source domain generalization. In *Proceedings of the IEEE conference on computer vision and pattern recognition*, pages 87–97, 2016. 2, 6
- [13] Junyu Gao, Tianzhu Zhang, and Changsheng Xu. I know the relationships: Zero-shot action recognition via two-stream graph convolutional networks and knowledge graphs. In *Proceedings of the AAAI Conference on Artificial Intelligence*, volume 33, pages 8303–8311, 2019. 6
- [14] Junyu Gao, Tianzhu Zhang, and Changsheng Xu. Learning to model relationships for zero-shot video classification. *IEEE Transactions on Pattern Analysis and Machine Intelligence*, 2020. 2, 8
- [15] Rohit Girdhar and Deva Ramanan. Attentional pooling for action recognition. In *Advances in Neural Information Processing Systems*, pages 34–45, 2017. 2
- [16] Rohit Girdhar, Deva Ramanan, Abhinav Gupta, Josef Sivic, and Bryan Russell. Actionvlad: Learning spatio-temporal aggregation for action classification. In *Proceedings of the IEEE Conference on Computer Vision and Pattern Recognition*, pages 971–980, 2017. 2

- [17] Shreyank N Gowda, Panagiotis Eustratiadis, Timothy Hospedales, and Laura Sevilla-Lara. Alba: Reinforcement learning for video object segmentation. *arXiv preprint arXiv:2005.13039*, 2020. 2
- [18] Yanli Ji, Yue Zhan, Yang Yang, Xing Xu, Fumin Shen, and Heng Tao Shen. A context knowledge map guided coarse-to-fine action recognition. *IEEE Transactions on Image Processing*, 29:2742–2752, 2019. 2
- [19] Zhong Ji, Yuxin Sun, Yunlong Yu, Jichang Guo, and Yanwei Pang. Semantic softmax loss for zero-shot learning. *Neurocomputing*, 316:369–375, 2018. 4
- [20] Elyor Kodirov, Tao Xiang, Zhenyong Fu, and Shaogang Gong. Unsupervised domain adaptation for zero-shot learning. In *Proceedings of the IEEE international conference on computer vision*, pages 2452–2460, 2015. 6
- [21] Hildegard Kuehne, Hueihan Jhuang, Estíbaliz Garrote, Tomaso Poggio, and Thomas Serre. Hmdb: a large video database for human motion recognition. In *2011 International Conference on Computer Vision*, pages 2556–2563. IEEE, 2011. 5, 6
- [22] Christoph H Lampert, Hannes Nickisch, and Stefan Harmeling. Learning to detect unseen object classes by between-class attribute transfer. In *2009 IEEE Conference on Computer Vision and Pattern Recognition*, pages 951–958. IEEE, 2009. 2
- [23] Aristidis Likas. A reinforcement learning approach to online clustering. *Neural computation*, 11(8):1915–1932, 1999. 4, 5
- [24] Bin Liu, Li Yao, Zheyuan Ding, Junyi Xu, and Junfeng Wu. Combining ontology and reinforcement learning for zero-shot classification. *Knowledge-Based Systems*, 144:42–50, 2018. 2
- [25] Changzhi Luo, Zhetao Li, Kaizhu Huang, Jiashi Feng, and Meng Wang. Zero-shot learning via attribute regression and class prototype rectification. *IEEE Transactions on Image Processing*, 27(2):637–648, 2017. 6
- [26] Laurens van der Maaten and Geoffrey Hinton. Visualizing data using t-sne. *Journal of machine learning research*, 9(Nov):2579–2605, 2008. 1
- [27] Devraj Mandal, Sanath Narayan, Sai Kumar Dwivedi, Vikram Gupta, Shuaib Ahmed, Fahad Shahbaz Khan, and Ling Shao. Out-of-distribution detection for generalized zero-shot action recognition. In *Proceedings of the IEEE Conference on Computer Vision and Pattern Recognition*, pages 9985–9993, 2019. 2, 6, 7, 8, 9, 10, 11
- [28] Pascal Mettes and Cees GM Snoek. Spatial-aware object embeddings for zero-shot localization and classification of actions. In *Proceedings of the IEEE International Conference on Computer Vision*, pages 4443–4452, 2017. 6
- [29] Tomas Mikolov, Ilya Sutskever, Kai Chen, Greg S Corrado, and Jeff Dean. Distributed representations of words and phrases and their compositionality. In *Advances in neural information processing systems*, pages 3111–3119, 2013. 5
- [30] Ashish Mishra, Anubha Pandey, and Hema A Murthy. Zero-shot learning for action recognition using synthesized features. *Neurocomputing*, 390:117–130, 2020. 7, 8
- [31] Ashish Mishra, Vinay Kumar Verma, M Shiva Krishna Reddy, S Arulkumar, Piyush Rai, and Anurag Mittal. A generative approach to zero-shot and few-shot action recognition. In *2018 IEEE Winter Conference on Applications of Computer Vision (WACV)*, pages 372–380. IEEE, 2018. 7, 8
- [32] Sanath Narayan, Akshita Gupta, Fahad Shahbaz Khan, Cees GM Snoek, and Ling Shao. Latent embedding feedback and discriminative features for zero-shot classification. *arXiv preprint arXiv:2003.07833*, 2020. 9
- [33] Juan Carlos Nibbles, Chih-Wei Chen, and Li Fei-Fei. Modeling temporal structure of decomposable motion segments for activity classification. In *European conference on computer vision*, pages 392–405. Springer, 2010. 6
- [34] Junhyuk Oh, Satinder Singh, Honglak Lee, and Pushmeet Kohli. Zero-shot task generalization with multi-task deep reinforcement learning. In *International Conference on Machine Learning*, pages 2661–2670, 2017. 2
- [35] Matteo Pagliardini, Prakhhar Gupta, and Martin Jaggi. Unsupervised learning of sentence embeddings using compositional n-gram features. In *Proceedings of NAACL-HLT*, pages 528–540, 2018. 5
- [36] Jie Qin, Li Liu, Ling Shao, Fumin Shen, Bingbing Ni, Jiaxin Chen, and Yunhong Wang. Zero-shot action recognition with error-correcting output codes. In *Proceedings of the IEEE Conference on Computer Vision and Pattern Recognition*, pages 2833–2842, 2017. 2, 6
- [37] Zhaofan Qiu, Ting Yao, and Tao Mei. Learning spatio-temporal representation with pseudo-3d residual networks. In *proceedings of the IEEE International Conference on Computer Vision*, pages 5533–5541, 2017. 2
- [38] Marcus Rohrbach, Michaela Regneri, Mykhaylo Andriluka, Sikandar Amin, Manfred Pinkal, and Bernt Schiele. Script data for attribute-based recognition of composite activities. In *Eur. Conf. Comput. Vis.*, 2012. 2
- [39] Bernardino Romera-Paredes and Philip Torr. An embarrassingly simple approach to zero-shot learning. In *International Conference on Machine Learning*, pages 2152–2161, 2015. 2
- [40] Yutaro Shigeto, Ikumi Suzuki, Kazuo Hara, Masashi Shimbo, and Yuji Matsumoto. Ridge regression, hubness, and zero-shot learning. In *Joint European Conference on Machine Learning and Knowledge Discovery in Databases*, pages 135–151. Springer, 2015. 6
- [41] Karen Simonyan and Andrew Zisserman. Two-stream convolutional networks for action recognition in videos. In *Advances in neural information processing systems*, pages 568–576, 2014. 2
- [42] Khurram Soomro, Amir Roshan Zamir, and Mubarak Shah. Ucf101: A dataset of 101 human actions classes from videos in the wild. *arXiv preprint arXiv:1212.0402*, 2012. 6
- [43] Du Tran, Lubomir Bourdev, Rob Fergus, Lorenzo Torresani, and Manohar Paluri. Learning spatiotemporal features with 3d convolutional networks. In *Proceedings of the IEEE international conference on computer vision*, pages 4489–4497, 2015. 2
- [44] Catherine Wah, Steve Branson, Peter Welinder, Pietro Perona, and Serge Belongie. The caltech-ucsd birds-200-2011 dataset. 2011. 6

- [45] Xiaolong Wang, Ross Girshick, Abhinav Gupta, and Kaiming He. Non-local neural networks. In *Proceedings of the IEEE conference on computer vision and pattern recognition*, pages 7794–7803, 2018. 2
- [46] Yongqin Xian, Tobias Lorenz, Bernt Schiele, and Zeynep Akata. Feature generating networks for zero-shot learning. In *Proceedings of the IEEE conference on computer vision and pattern recognition*, pages 5542–5551, 2018. 7, 8, 9, 10, 11
- [47] Yongqin Xian, Bernt Schiele, and Zeynep Akata. Zero-shot learning-the good, the bad and the ugly. In *Proceedings of the IEEE Conference on Computer Vision and Pattern Recognition*, pages 4582–4591, 2017. 6
- [48] Yongqin Xian, Bernt Schiele, and Zeynep Akata. Zero-shot learning-the good, the bad and the ugly. In *Proceedings of the IEEE Conference on Computer Vision and Pattern Recognition*, pages 4582–4591, 2017. 7
- [49] Yongqin Xian, Saurabh Sharma, Bernt Schiele, and Zeynep Akata. f-vaegan-d2: A feature generating framework for any-shot learning. In *Proceedings of the IEEE/CVF Conference on Computer Vision and Pattern Recognition*, pages 10275–10284, 2019. 9
- [50] Jianxiong Xiao, James Hays, Krista A Ehinger, Aude Oliva, and Antonio Torralba. Sun database: Large-scale scene recognition from abbey to zoo. In *2010 IEEE computer society conference on computer vision and pattern recognition*, pages 3485–3492. IEEE, 2010. 6
- [51] Guo-Sen Xie, Li Liu, Fan Zhu, Fang Zhao, Zheng Zhang, Yazhou Yao, Jie Qin, and Ling Shao. Region graph embedding network for zero-shot learning. In *European Conference on Computer Vision*, pages 562–580. Springer, 2020. 9, 10
- [52] Xun Xu, Timothy Hospedales, and Shaogang Gong. Transductive zero-shot action recognition by word-vector embedding. *International Journal of Computer Vision*, 123(3):309–333, 2017. 2, 6
- [53] Xun Xu, Timothy M Hospedales, and Shaogang Gong. Multi-task zero-shot action recognition with prioritised data augmentation. In *European Conference on Computer Vision*, pages 343–359. Springer, 2016. 2
- [54] Zhiquan Ye, Yuxia Geng, Jiaoyan Chen, Jingmin Chen, Xiaoxiao Xu, SuHang Zheng, Feng Wang, Jun Zhang, and Huajun Chen. Zero-shot text classification via reinforced self-training. In *Proceedings of the 58th Annual Meeting of the Association for Computational Linguistics*, pages 3014–3024, 2020. 2
- [55] Li Zhang, Tao Xiang, and Shaogang Gong. Learning a deep embedding model for zero-shot learning. In *Proceedings of the IEEE Conference on Computer Vision and Pattern Recognition*, pages 2021–2030, 2017. 3
- [56] Yi Zhu, Yang Long, Yu Guan, Shawn Newsam, and Ling Shao. Towards universal representation for unseen action recognition. In *Proceedings of the IEEE Conference on Computer Vision and Pattern Recognition*, pages 9436–9445, 2018. 2, 6